

## ARTICLE OPEN



# Identification and quantification of giant bioaerosol particles over the Amazon rainforest

Cybelli G. G. Barbosa<sup>1,2,3</sup>✉, Philip E. Taylor<sup>4</sup>, Marta O. Sá<sup>5</sup>, Paulo R. Teixeira<sup>5</sup>, Rodrigo A. F. Souza<sup>6</sup>, Rachel I. Albrecht<sup>7</sup>, Henrique M. J. Barbosa<sup>8,9</sup>, Bruna Sebben<sup>10</sup>, Antônio O. Manzi<sup>10</sup>, Alessandro C. Araújo<sup>11</sup>, Maria Prass<sup>1</sup>, Christopher Pöhlker<sup>1</sup>, Bettina Weber<sup>1,3</sup>, Meinrat O. Andreae<sup>1,12</sup> and Ricardo H. M. Godoi<sup>2</sup>✉

Eukarya dominate the coarse primary biological aerosol (PBA) above the Amazon rainforest canopy, but their vertical profile and seasonality is currently unknown. In this study, the stratification of coarse and giant PBA >5 µm were analyzed from the canopy to 300 m height at the Amazon Tall Tower Observatory in Brazil during the wet and dry seasons. We show that >2/3 of the coarse PBA were canopy debris, fungal spores commonly found on decaying matter were second most abundant (ranging from 15 to 41%), followed by pollens (up to 5%). The atmospheric roughness layer right above the canopy had the greatest giant PBA abundance. Measurements over 5 years showed an increased abundance of PBA during a low-rainfall period. Giant particles, such as pollen, are reduced at 300 m, suggesting their limited dispersal. These results give insights into the giant PBA emissions of this tropical rainforest, and present a major step in understanding the type of emitted particles and their vertical distribution.

*npj Climate and Atmospheric Science* (2022)5:73; <https://doi.org/10.1038/s41612-022-00294-y>

## INTRODUCTION

Primary biological aerosols (PBA) including bacteria, fungi, fern and bryophyte spores, viruses, fragments of insects and leaves are abundant in the atmosphere and are agents for the spread of microorganisms and reproductive material, ranging in size from a few nanometers up to several millimeters<sup>1–4</sup>. In the Amazon, air sampling above and below the canopy has shown that fungal spores dominate the coarse size range of suspended particles<sup>3,5</sup>. About 90% of atmospheric particles <10 µm are composed of organic material, irrespective of the season<sup>5–8</sup>.

In a recent wet-season study using fluorescence insitu hydridization, coarse PBA were dominated by bacteria and Eukaryotes, and the largest of these were greatly reduced at 300 m height. Also, up to 30% of coarse PBA were attributed to biological debris<sup>9</sup>.

The smallest of the suspended particles are mostly secondary organic aerosols, known to scatter and absorb radiation and initiate the formation of clouds and precipitation by acting as cloud condensation and ice nuclei<sup>6,10–13</sup>. It also was suggested that a significant part of smaller particles originated from primary emission, i.e., fungal discharge liquids and fragmented spores<sup>14,15</sup>. In tropical regions, the regional circulation pattern and evapotranspiration, together with bioaerosols, are important factors shaping hydrological processes<sup>16–19</sup>.

The potential for vertical transport of coarse PBA and the role they might play in cloud formation has been frequently discussed. Some authors point out that PBA can act as giant (usually >10 µm<sup>2</sup>) CCN in the atmosphere, whereby water condenses on a large particle, producing a tail of large droplets with high collection efficiency, enhancing collision and

coalescence processes, and influencing warm rain formation<sup>20–22</sup>. Thus, it is important to identify the sources and measure the abundance of coarse PBA that are carried above the rainforest canopy in order to estimate the PBA contribution to CCN above the Amazon forest.

Vertical atmospheric lifting is a prerequisite for long-range transport of aerosols and is related to and controlled by pressure systems, convection and inversion layers<sup>23</sup>. Coarse PBA have been reported to travel across countries and the ocean, but these are believed to be rare events<sup>24</sup>. Daily regional forecast models for atmospheric pollen abundance still assume an even distribution from near ground level to the top of the atmospheric boundary layer, i.e., to a height of ~1 km above ground level<sup>25–27</sup>. However, many studies on the distribution of pollen grains up to 100 m above ground showed that their abundance was well-correlated with specific meteorological conditions<sup>25,26,28–31</sup>. Using aircraft measurements, high concentrations of aerosol particles were reported to be transported across the boundary layer by strong convection<sup>30</sup>. However, there is a paucity of long-term studies on PBA particles at fixed heights and especially in tropical regions. In the central Amazon rainforest, there are strong updrafts and downdrafts from frequent deep convection events that could influence vertical PBA transport.

In the current study, we conducted long-term tower-based measurements at 5 height levels up to 300 m above ground to identify coarse and giant PBA >5 µm in the Amazon rainforest atmosphere. This profile was linked to meteorological data to infer the seasonality effects on PBA vertical gradients.

<sup>1</sup>Multiphase Chemistry and Biogeochemistry Departments, Max Planck Institute for Chemistry (MPIC), Mainz, Germany. <sup>2</sup>Environmental Engineering Department, Federal University of Paraná (UFPR), Curitiba, PR, Brazil. <sup>3</sup>Institute for Biology, Division of Plant Sciences, University of Graz, Graz, Austria. <sup>4</sup>Department of Pharmacy and Biomedical Sciences, La Trobe Institute for Molecular Science, La Trobe University, Bendigo, VIC, Australia. <sup>5</sup>Large Scale Biosphere-Atmosphere Experiment in Amazonia (LBA), Instituto Nacional de Pesquisas da Amazonia (INPA), Manaus, AM, Brazil. <sup>6</sup>Meteorology Department, State University of Amazonas (UEA), Manaus, AM, Brazil. <sup>7</sup>Institute of Astronomy, Geophysics and Atmospheric Sciences (IAG), University of São Paulo (USP), São Paulo, SP, Brazil. <sup>8</sup>Institute of Physics, University of São Paulo (USP), São Paulo, SP, Brazil. <sup>9</sup>Department of Physics, University of Maryland Baltimore County (UMBC), Baltimore, MD, USA. <sup>10</sup>National Institute for Space Research (INPE), São José dos Campos, SP, Brazil. <sup>11</sup>Empresa Brasileira de Pesquisa Agropecuária (EMBRAPA), Belém, PA, Brazil. <sup>12</sup>Scripps Institution of Oceanography, University of California San Diego, La Jolla, CA, USA. <sup>✉</sup>email: c.barbosa@mpic.de; rhmgodoi@ufpr.br

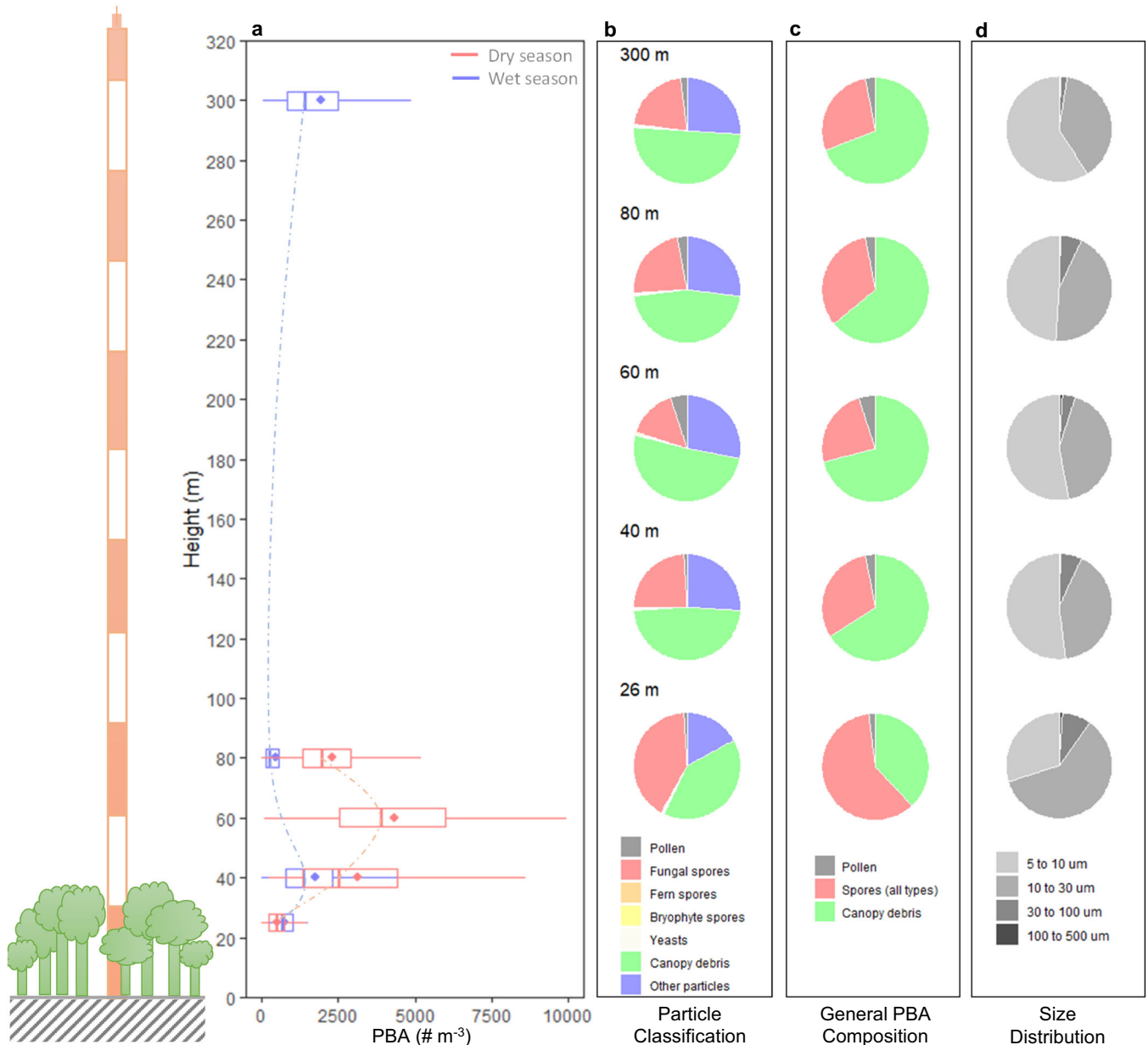


**Fig. 1 Vertical distribution and composition of giant PBA.** Particles ranging from 5 to 500  $\mu\text{m}$  at 5 different heights above the Amazon rainforest: 26 m, 40 m, 60 m, 80 m, and 300 m. Data at each height are confined to the sampling periods at the respective level (see Table 1). **a** Seasonal PBA quantification and general profile. Boxplots with the representation of the box for the 1st and 3rd quartiles, vertical line inside the box shows the median value, while the dot indicates the average value, 5 and 95 percentiles as whiskers. Dry season displayed in red and wet season in blue; **b** Detailed particle classification per height with relative contribution of each category as displayed in the legend; **c** General PBA composition with the following categories merged as spores: fungal spores, fern spores, bryophyte spores, yeasts; **d** Size distribution of PBA particles from 5 to <10  $\mu\text{m}$ , 10 to <30  $\mu\text{m}$ , 30 to <100  $\mu\text{m}$ , and 100 to 500  $\mu\text{m}$ .

## RESULTS AND DISCUSSION

### Identification and classification of coarse aerosol

All coarse aerosol particles >5  $\mu\text{m}$  collected in air samples at 5 different heights above ground level (26, 40, 60, 80, 300 m) were classified as either PBA (pollen grains, fungal spores, yeast-like spores, fern spores, bryophyte spores, canopy debris) or other particles (smoke, mineral fractions). Above the rainforest canopy, coarse particles numbers were dominated by diverse non-reproductive biological parts (leaf/wood pieces, plant waxes, leaf glands, leaf trichomes, insect fragments), classified as canopy debris (Fig. 1, Supplementary Fig. 1). These debris particles covered the widest range of sizes and shapes and represented >2/3 of all sampled particles at the different heights above the

canopy (Supplementary Fig. 1), representing 40% of the sampled particles at 26 m, 48% at 40 m, 51% at 60 m, 46% at 80 m and 50% at 300 m. At the canopy level (26 m), spores played a similarly large role, representing 41% of the particles, decreasing with height to 24, 15, 23 and 21% at 40, 60, 80 and 300 m respectively.

The abundance of pollen grains represented about 2% of coarse PBA at all levels, with the highest fraction of 5% reached at 60 m height. Fern spores represented <1% of particles identified (0.1, 0.2, 0.5, 0.3 and 0.2% at 26, 40, 60, 80 and 300 m, respectively) and only a few spore types were present (Fig. 1).

Bryophyte spores were rarely observed (<0.1% at all heights), and these were mainly located within the canopy (26 m height). Small hyaline, thin-walled spores similar to the blastoconidia of

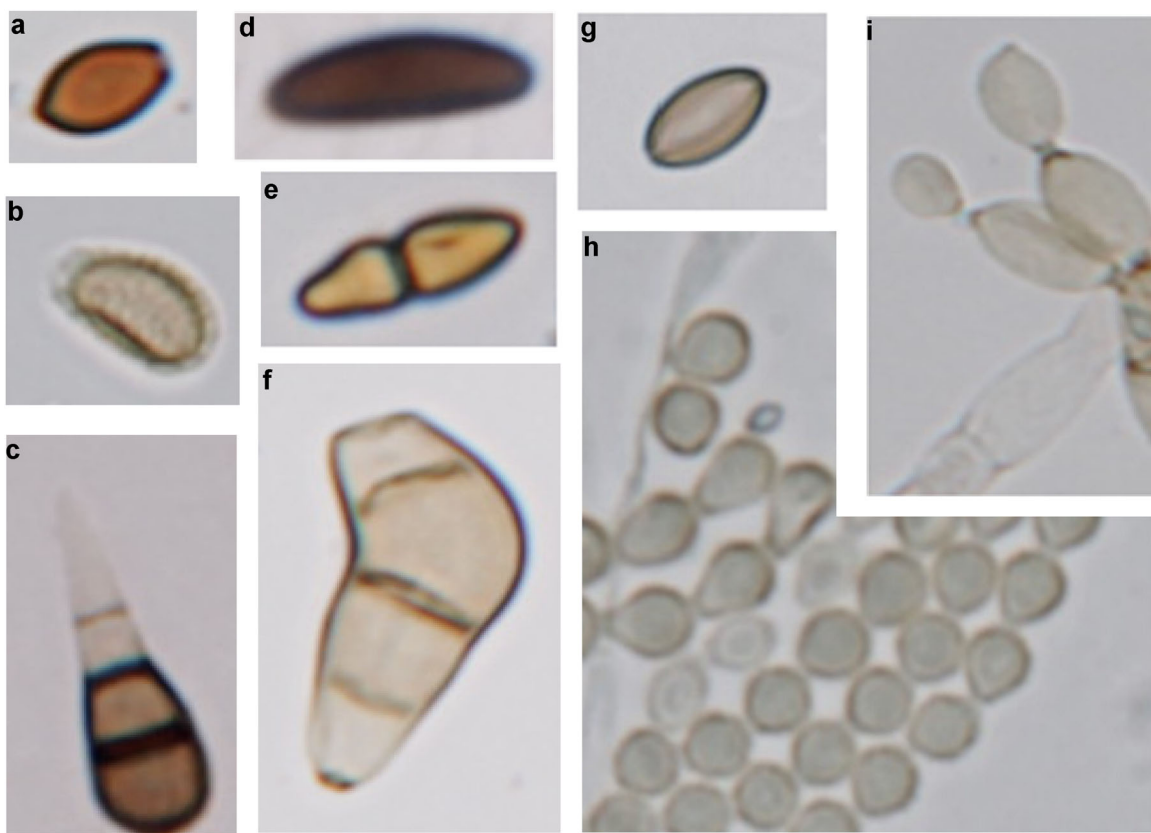


**Fig. 2 Images of common fungal spores sampled at the different heights over the rainforest and identified up to family level.** **a** Agaricaceae, **b** Polyporaceae, **c** Pleosporaceae, **d** Xylariaceae, **e** Venturiaceae, **f** Pleosporaceae, **g** Agaricaceae, **h** Trichocomaceae, **i** Cladosporiaceae. Scale bar: 10 µm.

yeasts <10 µm were classified as yeast-like, and these were found across all heights and seasons, but represented <1% of the total particle number (0.8, 0.7, 0.4, 0.6 and 0.7% at 26, 40, 60, 80 and 300 m, respectively). They were sampled mostly prior to rain events. All the PBA subcategories were present at all sampled heights and seasons.

The general composition indicates an atmospheric dominance of fungi (around 1/4), and many of the identified spores (Fig. 2) belong to the saprophytes, associated with decaying organic material. Overall, the most common fungal spore identified was *Ganoderma*, a bracket fungus. Sexual spore release in these basidiomycetes is associated with the formation of the so-called Buller's Drop<sup>32</sup>, which causes the emission of a similar mass of propulsion liquid that is also aerosolized. This liquid likely causes the formation of salt-enriched aerosol particles of smaller size (mainly belonging to the accumulation mode)<sup>3,33</sup>.

Fungi showed the highest abundance among the spore producing organisms, from 15 to 41% depending on the height (Fig. 2b) as well as the greatest diversity of spore types, as showed in the Atlas<sup>34</sup>. Around 70% of the collected spores belonged to the Ascomycota or Basidiomycota, the remaining percentage belong to other fungal phyla, yeast, fern, or bryophyte organisms. The most common ascospores identified were from the Xylariaceae, Venturiaceae, Cladosporiaceae, Pleosporaceae and Trichocomaceae families (Fig. 2). For basidiospores, the Polyporaceae, followed by Agaricaceae and Bolbitiaceae families were most abundant across all heights (a unique result of this work is presented as an Image atlas<sup>34</sup> displaying the microscopic pictures of the biological particles collected above the canopy, available online (<https://doi.org/10.6084/m9.figshare.15142419.v1>).

Fungal spores and other spore particles were distributed across all sampling heights (Fig. 1c), but molecular or other techniques would be required for identification to species level. In a previous study in the Amazon, where measurements were conducted near the ground level, a similar relative composition was observed with fungal spores accounting for a major fraction, 45%, of the coarse particulate matter<sup>3</sup>.

Size measurement can be challenging for non-spherical particles. Minor and major axes were measured for each particle, these values were averaged and the standard deviation (sd) among minimum, maximum and mean values were analyzed. For pollen grains, where the sd was <10%, the average value was considered as the mean diameter, or just diameter along the text. For the remaining categories, the sd reached around 50%, and even higher values for fungal spores due to their diverse morphology. Here, the major axis was used to refer to the particle size.

Across all heights, the size of the sampled large PBA mainly ranged between 5 and 30 µm (Fig. 1d, Supplementary Fig. 2). A few large particles from the canopy measured up to 500 µm and were identified as insect and leaf parts.

Airborne pollen dominated the particle size fraction below 30 µm diameter (Supplementary Fig. 2, Supplementary Table 1), across all heights. Giant pollen grains, with sizes from 30 to 100 µm ranged among the largest known PBA particles<sup>35</sup>.

Across all heights, 80 different types of pollen were observed, and 25 families identified (Supplementary Table 1). The most abundant pollen were small grains from the Moraceae (Fig. 3e) family (measuring in the range from 8 to 20 µm, with an average diameter of 10 µm). Many species of Moraceae are wind-

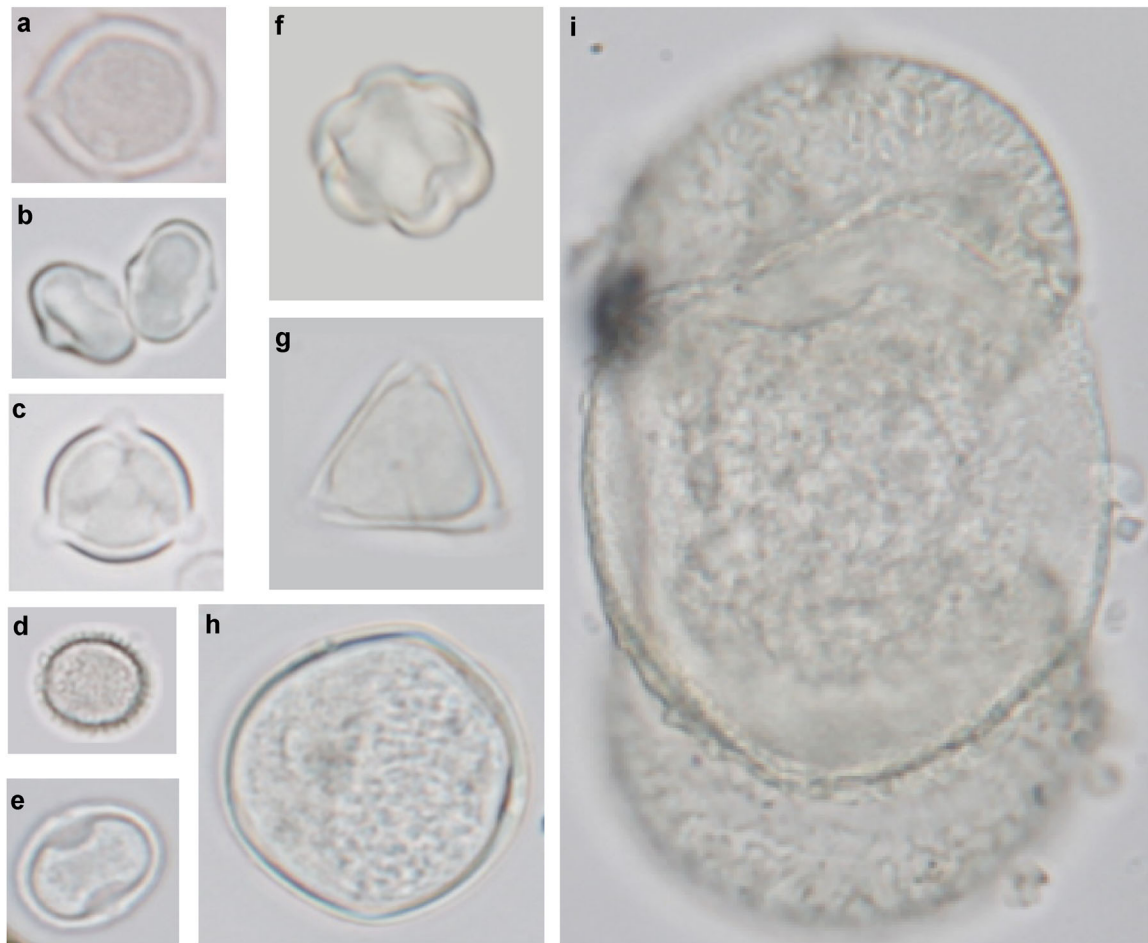


**Fig. 3 Images of common pollen grains sampled at the different heights over the rainforest and identified up to family level.** **a** Oleaceae, **b** Fabaceae, **c** Euphorbiaceae, **d** Asteraceae, **e** Moraceae, **f** Meliaceae, **g** Sapindaceae, **h** Poaceae, and **i** Podocarpaceae. Scale bar: 20  $\mu\text{m}$ .

pollinated, discharging their pollen forcibly in response to a drop in relative humidity (RH)<sup>36</sup>. Among the largest in size were pollen grains of a wind-pollinated tree in the Podocarpaceae family (Fig. 3i), present at 26, 60 and 80 m height. The remaining identified pollens (Supplementary Table 1) were from families more known for animal and insect pollination than wind pollination.

Some pollen grains are known to be capable of rupture, releasing their content into the atmosphere<sup>37</sup>. For temperate regions, up to 50% of pollen grains have been observed to be ruptured<sup>37–41</sup>. These pollen shells have been regularly observed in temperate cities during and after convective storms<sup>39,42</sup>. Their dispersed nanoparticle content has the potential for cloud nucleation, affecting warm precipitation, and secondary particle formation in the atmosphere<sup>40,41</sup>. Over the Amazon, in our study, only about 3% of pollen collected during a major storm showed obvious wall collapse and an absence of cytoplasmic contents (Supplementary Fig. 3). We triggered grass pollen rupture in the laboratory (Supplementary Fig. 3) and used microscopic imaging of these pollen shells as a reference material. Outside of storm events, ruptured pollen shells were rarely observed in our samples.

The pollen rupture events, across all heights and seasons, were analyzed by means of air mass back trajectories, and tested for potential correlations with the presence and number of lightning strikes and meteorological parameters up to 72 h prior to sampling. However, no pattern or tendency was found, which could explain these few rupture events.

Although time-consuming, the optical microscopy technique used for particle classification provides relevant information on shape, size and morphological<sup>34</sup> characterization, allowing a more detailed assessment of the relative composition, both time-resolved and along the vertical profile.

#### PBA quantification and vertical distribution

The main focus was to identify the relative similarities/differences along the vertical gradient and explore the general upward trend from the canopy. Starting within the canopy, at 26 m height above ground level, relative humidity had a weak to moderate correlation with biological particles (Supplementary Fig. 4), despite remaining above 80% for at least 70% of the sampling period during the wet and dry seasons (Supplementary Fig. 5). Also, horizontal wind speeds were much lower than above canopy, generally not exceeding  $5 \text{ m s}^{-1}$  (Supplementary Fig. 1), and not directly influencing particle dispersal (Spearman:  $-0.25 < \rho < 0.1$ ,  $p < 0.001$ ). At this level the main difference was the reduction of the canopy debris during the wet season (Fig. 4a), a common trend due to the washout effect, and an increased concentration of spores (mostly from fungal organisms, but also fern and bryophytes) expected due to the proximity of the source, heavily influenced the PBA relative composition ( $\rho = 0.94$ ,  $p < 0.001$ ).

This was the only level that showed statistical day/night differences for spores and PBA distribution ( $p < 0.001$ ) (Supplementary Table 2). Daylight and nighttime have nearly similar

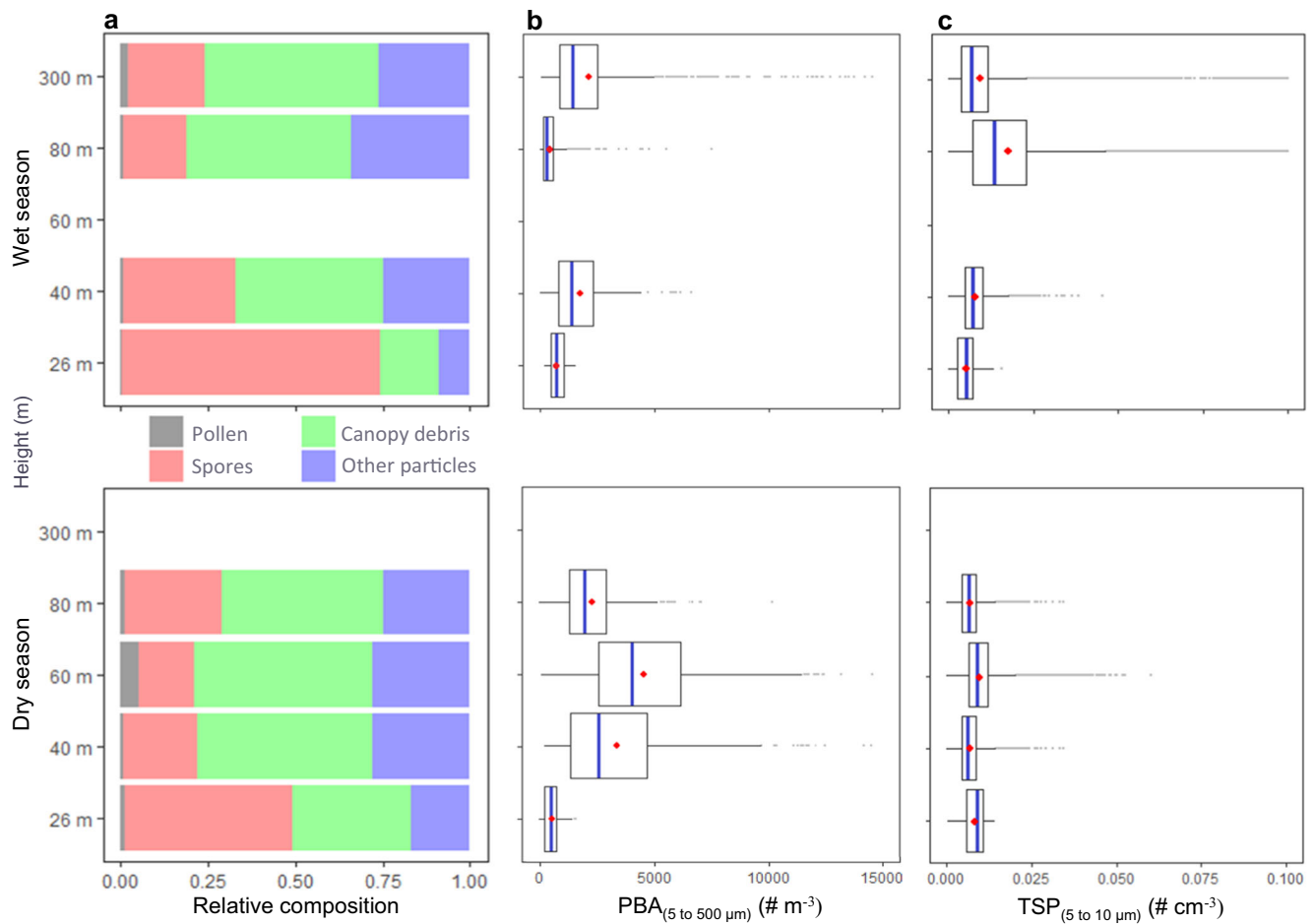


**Fig. 4 General seasonal distribution and particle quantification per height and season (wet season: top, dry season: bottom).** **a** Relative composition of all sampled particles per height and season presenting the main categories: pollen, all spores, canopy debris and other particles in gray, red, green and blue respectively; **b** PBA (5 to 500  $\mu\text{m}$ ) concentration ( $\# \text{ m}^{-3}$ ) as boxplots for each height and season with the box for 1st and 3rd quartiles, median as a blue line and mean as the red dot, 5 and 95 percentiles as whiskers, outliers marked as gray dots; **c** total suspended particle concentration in the range from (5 to 10  $\mu\text{m}$ ) ( $\# \text{ m}^{-3}$ ) also shown for each height and level, with the presence of more outliers during the wet season for the highest levels.

length period at the region along the year. The almost homogeneous day/night distribution for biological particles above canopy level is consistent with results obtained in 2001 in a forest clearing<sup>43</sup>.

At 40 m, the general pattern followed the level immediately below (Supplementary Fig. 6). Spores still contributed to PBA composition, especially during the wet season (Fig. 4a), with a moderate correlation ( $\rho = 0.6$ ,  $p < 0.001$ ) between spores and total PBA concentrations (Supplementary Fig. 4). But canopy debris contribute a larger amount (Fig. 1c), similar to the levels above. Particles of pollen, ferns and many fungi require a drop in RH to trigger emission (considering a previously condensed atmosphere), as well as a minimum threshold of wind disturbance for dispersion, therefore these categories presented a significant distribution difference between wet and dry seasons ( $p < 0.001$ ) (Supplementary Table 2), with higher values during the dry season. Also, pollen grains rapidly condense moisture above 90% RH.

The 60 m level showed the highest PBA concentrations (Fig. 1a, Supplementary Fig. 7). Overall, the elevated values, compared to the other heights has to be considered in the context of the extreme dry climatic conditions during this sampling period: few rain events with low precipitation levels and high temperatures for longer periods. The sampling height of 60 m above ground level was just above the roughness layer, where the turbulent flows above the canopy are not yet well established<sup>44,45</sup>, and none of

the monitored meteorological parameters presented a strong correlation with the sampled biological particles at this level (Supplementary Fig. 4).

High variability in relative humidity (Supplementary Fig. 7), reduced precipitation and occurrence of gusts (Supplementary Fig. 1) might influence particle resuspension and increased PBA availability.

At the level of 80 m, there was higher abundance of spores during the dry season (Fig. 4a, Supplementary Table 2). The washout effect could have prevailed during the wet season, and thunderstorms were present that entrain a diversity of particles due to atmospheric turbulence (Supplementary Fig. 8).

The same pattern of relative spore abundance also occurred at 300 m (Fig. 1b), indicating that the local contribution from the canopy predominates at this level. Only a PBA peak at 300 m that occurred during the wet season could be associated with long-range transport (Supplementary Fig. 9). Organic particles usually have ornamented external walls, lower density, and shapes that favor dispersion. After being entrained from the canopy, coarse and giant PBA can accumulate in the roughness layer, but this is highly dependent on the settling time of each particle.

#### Seasonality and long-range transport

Despite persistent high relative humidity in the Amazon (Supplementary Fig. 1), PBA were entrained above the rainforest

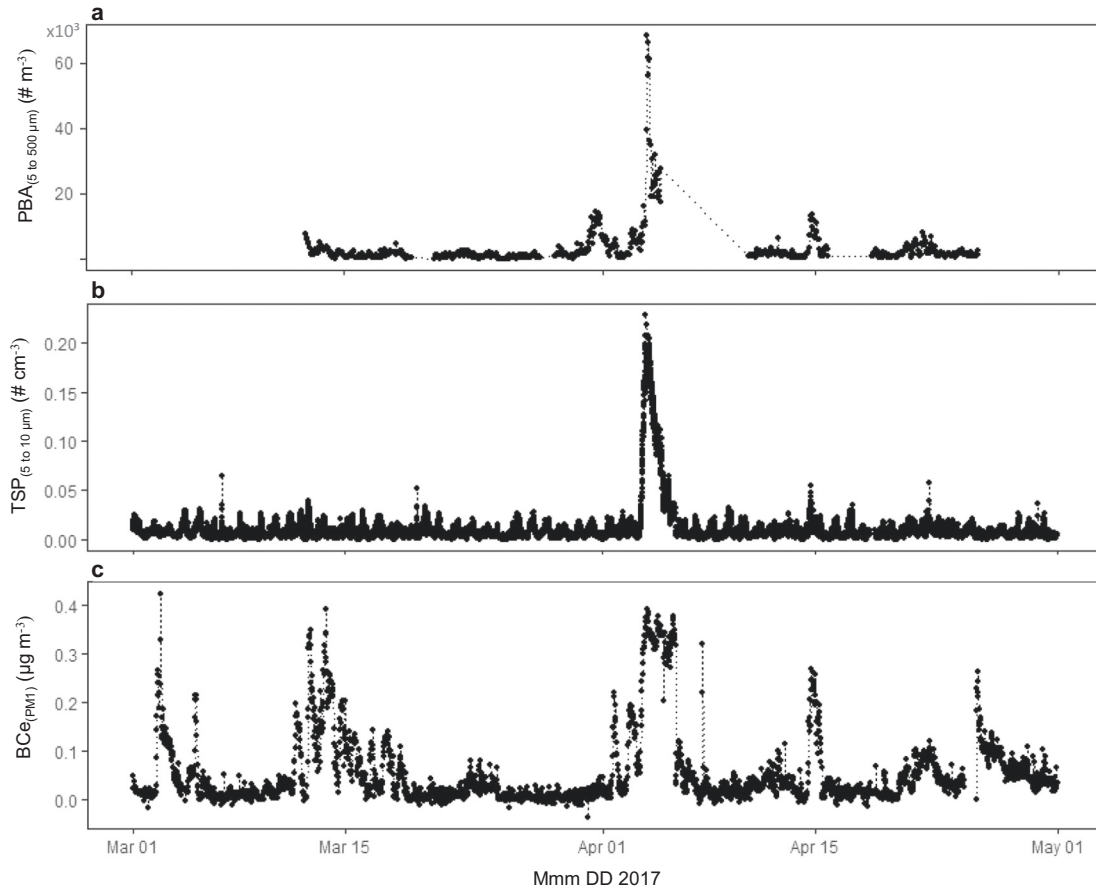


**Fig. 5 High PBA concentrations observed during the wet season at 300 m when reduced local emissions are often registered.** The sampled peak in particles (a) from 5 to 500  $\mu\text{m}$  follows the same pattern seen in the narrow range (b) 5–10  $\mu\text{m}$ ; c equivalent black carbon highlights the smoke contribution.

canopy throughout both the wet and dry seasons. Precipitation reached a minimum in August and peaked in March across all years sampled, consistent with previous records in the same area<sup>46</sup>. Detailed PBA data for each season and at each of the sampled heights were compared with meteorological data. Higher T values were observed at the end of 2015 and the beginning of 2016 (Supplementary Figs. 1 and 8), consistent with reduced precipitation<sup>9</sup>. Mean wind speed values were almost constant across the years, around  $3 \text{ m s}^{-1}$  at all levels, with gusts above  $11 \text{ m s}^{-1}$  (Supplementary Fig. 1), promoting mixture and particle resuspension.

Thunderstorms have an effect on coarse PBA drag above tree level. Peaks in large PBA (30 to 100  $\mu\text{m}$ ) abundance above the canopy coincident with wind gusts (Supplementary Fig. 3) from the outflow of convective storms are common during the transition between wet and dry seasons. Two storms were monitored<sup>24</sup> and associated strong winds entrained the largest of pollen grains and other bioaerosols above the canopy, enabling their potential transport over larger distances. At 80 and 300 m height, wind speed was positively correlated with PBA concentration ( $p < 0.01$ ) only during storm events, while for the general period there was no significant correlation (Supplementary Table 2). This implies that storm-like disturbances are key for enhanced transport of coarse and giant PBA. Convective storms resulted in short discrete plumes of PBA. Subsequent precipitation and increased relative humidity had a strong negative influence on the vertical distribution of bioaerosols, with a reduction in the number of PBA.

The atypical peak (Fig. 5a) during the wet season, in a pristine area, might be a result of multiple influences during a period when reduced emissions are usually registered. The event coincided with a peak in the coarse mode particles from 5 to 10  $\mu\text{m}$  (Fig. 5b). Only local emissions do not explain the high number of particles recorded, and the equivalent black carbon mass concentration (Fig. 5c) shows an increase at this time during the wet season in the Amazon, when the local fire contribution is not significant. This pattern was previously described for small particles as resulting from long-range transport of Saharan dust aerosol mixed with pyrogenic aerosols from West Africa<sup>47</sup>. The peak observed across all size ranges during this specific period could be influenced by a resuspension component combined with local emission and intercontinental input.

A few pollen grains were identified above canopy from species that grow near ground level. Pollen of Poaceae (Fig. 3) was occasionally observed at 80 m. This was subsequently identified as bamboo (*Pariana* sp.). This genus is common on the forest floor and was thought to have fully adapted to insect pollination. There appears to be insufficient disturbance for these pollen types to escape an intact canopy. However, several observations of Cyperaceae pollen above the canopy provide support to the likelihood of small emission contributions from clearings or riverbanks.

Consistently high levels of PBA observed during the dry season might be driven by a combination of variable dispersal, connected to environmental and meteorological variables<sup>47</sup>. The smallest particles (5–10  $\mu\text{m}$ ) were the most abundant across the coarse and giant particle number size distribution. Above the canopy, the

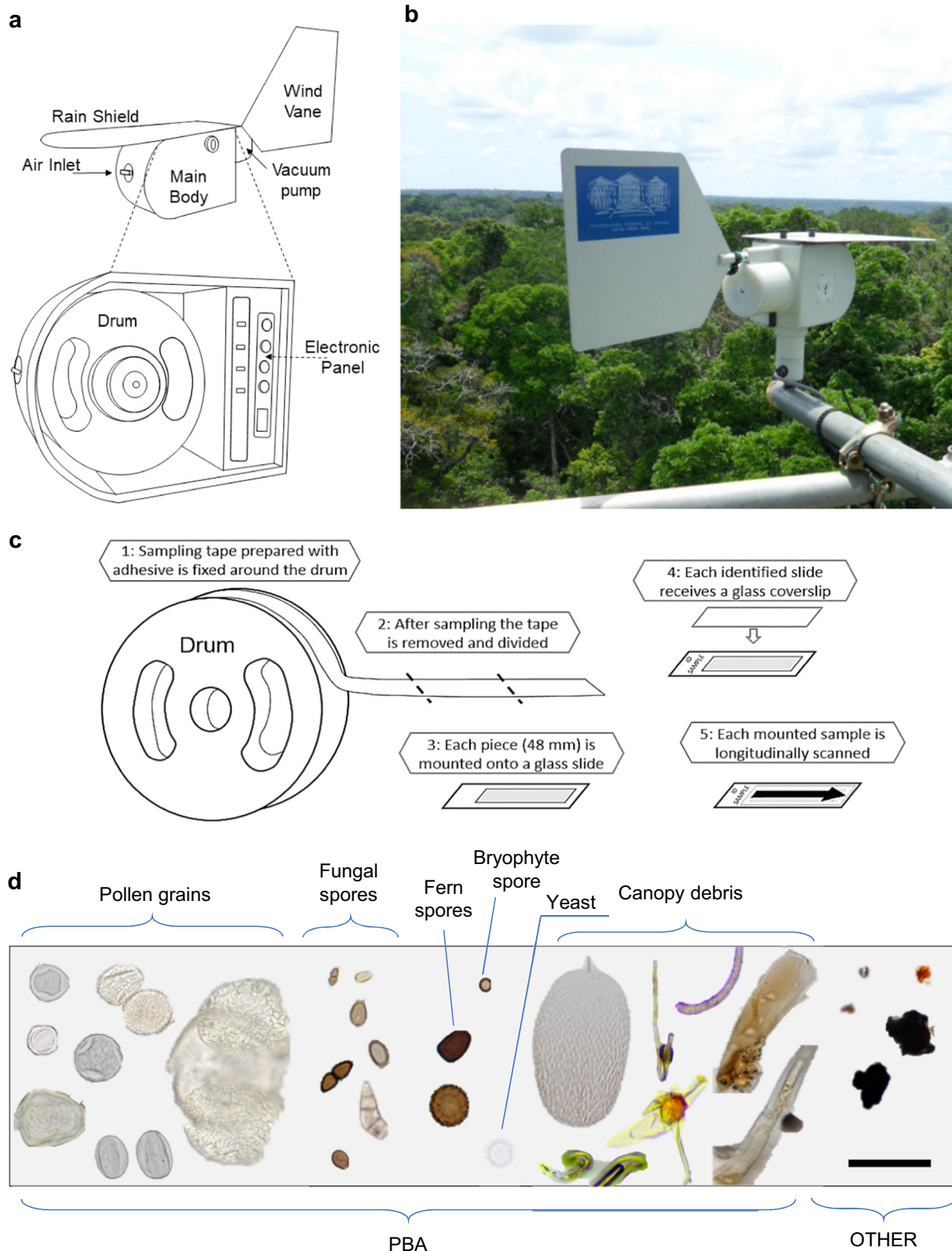


**Fig. 6 Equipment and method of sampling.** **a** Drawing scheme of the Burkard Volumetric Spore Sampler describing the parts attached to the main body, with the internal view in detail showing the rotating drum; **b** Picture of the sampler attached to the tower by a metallic support allowing free rotation according to the wind direction; **c** Scheme of the steps followed during sampling: (1) sampling tape preparation with adhesive along the entire surface and fixation on the side of the rotating drum, (2) removal of the tape after sampling and separation into pieces, (3) mounting of each piece onto a glass slide, (4) application of coverslip on top, (5) longitudinal scanning under an optical microscope allowing time discrimination (1-h resolution); **d** example of sampled slide with all the categories: PBA (pollen grain, fungal spore, fern spore, bryophyte spore, yeast, canopy debris) and Other particles. Scale bar: 50 µm.

**Table 1.** Sampling calendar, describing the period (month and year), height (meters above ground level: 26, 40, 60, 80, 300 m) and season (dry or wet) of each sampling campaign.

Year	2015	2015	2016	2016	2017	2018	2019
Months	JAN MAR APR	SEP OCT NOV	SEP OCT	NOV DEC	MAR APR	AUG	MAR
Season	WET	DRY	DRY	WET	WET	DRY	WET
Height	80	60	40	40	300	26	26
			80	300			

seasonality and mixing layer can influence the concentration, increasing or diluting local emissions<sup>48</sup>.

In a tropical lowland forest in Costa Rica, seasonal influences had a strong effect on the canopy habitat<sup>49</sup>. The dry season correlated with a build-up of tree leaf litter and increased canopy soil. During other seasons, rainfall and associated winds regularly scrubbed the canopy. High abundance of coarse PBA above the Amazon canopy observed during the dry season could be due to decreased rainfall leading to increased retention of dead organic matter within the canopy. This would cause an increased availability of amorphous particles and saprophytic fungal spores to be released into the atmosphere.

Canopy particles were quantified as the major contributor of coarse PBA in the size range of 5 to 500 µm above the canopy, followed by fungal spores across all heights and seasons. Air sampling of the pristine atmosphere of the Amazon rainforest suggests that the canopy habitat is the source of emission of most coarse PBA, mostly emitted as amorphous canopy particles and fungal spores, with minor abundance of pollen grains.

Besides the quantitative limitation of the optical microscopy technique, our dataset allows an enhanced qualitative discrimination and classification of PBA particles within and over the canopy. The vertical composition from the canopy up to 300 m height highlights the most abundant categories that are representative for both seasons.

As PBA dispersion, despite the climatic effect, might be important for forest conservation, more studies would be required to connect the consequences of the production, emission and viability of large biological particles, and the role of canopy particles on the balance of the Amazon ecosystem. A continuous vertical large-PBA measurement could provide important parameters to better understand the natural processes driven by seasonality and also improve numeric models of the tropical region.

## METHODS

### Sampling

Sampling was conducted at the Amazon Tall Tower Observatory (ATTO) in the Uatumã Sustainable Development Reserve (RDS Uatumã), located in the Amazonas state, Brazil<sup>8</sup>. Two towers were used to run air samplers at different heights: the INSTANT tower ( $S = 2^{\circ} 8.647' W = 58^{\circ} 59.992'$ ) with sampling at the canopy level (26 m), and above canopy (40, 60 and 80 m), and the ATTO tower ( $S = 2^{\circ} 8.752' W = 59^{\circ} 0.335'$ ) with sampling at 300 m height above ground level. The sampling of coarse airborne particles was performed using two Hirst-type volumetric samplers<sup>50,51</sup> (Burkard 7-Day Recording Volumetric Spore Samplers, Burkard Scientific Ltd., Uxbridge, UK). The sampler cut-point allowed the collection of particles from 3 to 2000 µm in size, and only the particles from 5 to 500 µm were considered for this study. Samplers were installed with a metallic arm support allowing the main body to be placed outside the tower and freely rotate according to the wind direction (Fig. 6). Sampling was performed during both the wet and dry seasons of several subsequent years (Jan, Sep, Oct and

Nov of 2015; Sep, Oct, Nov and Dec 2016; Mar and Apr 2017; Aug 2018 and Mar 2019) and at different sampling heights (Table 1), with a total of 4737 h of sampling distributed as follows: 192 h at 26 m, 621 h at 40 m, 1316 h at 60 m, 1394 h at 80 m and 1214 h at 300 m.

The Amazon region presents characteristic dry and rainy (wet) seasons, interspersed by transition periods. For this study the entire sampling period was separated only into dry and wet seasons (Table 1) according to the monthly precipitation levels<sup>52</sup>.

Additionally, data from an Optical Particle Sizer (OPS, model 3330, TSI Inc. Shoreview, MN, USA), from 5 to 10 µm in size at 60 m height, and from a Multi-Angle Absorption Photometer (MAAP, model 5012, Thermo Electron Group, Waltham, USA) were used for coarse particle number concentration and equivalent black carbon concentration, respectively.

### Meteorological data

Meteorological data for 26, 40, 60 and 80 m (sampling periods of 2015, 2016, 2018 and 2019) were obtained from the closest sensors installed along an 81 m-height tower, i.e., 26, 40, 55 and 81 m, respectively. Air Temperature and relative humidity (CS215, Rotronic Measurement Solutions, UK), wind speed and direction (2D/3D sonic anemometers (WindSonic, Gill Instruments Ltd., UK)) for the mentioned levels, while rainfall (TB4, Hydrological Services Pty. Ltd., Australia) just at 81 m height. The 1-min data for the above-mentioned parameters were averaged to be comparable with the 1-h PBA concentration resolution. Meteorological data for 300 m height was estimated based on radiosonde data measurements (for the years of 2016 and 2017, launched daily from  $S = 3^{\circ} 2.316' W = 60^{\circ} 2.982'$ ), as there were still no meteorological instruments installed at that level during this sampling period. The National Oceanic and Atmospheric Administration (NOAA) Air Resources Laboratory (ARL) HYSPLIT Trajectory Model (HYbrid Single-Particle Lagrangian Integrated Trajectory) was used for computing air parcel 24, 48, and 72 h back trajectories (<http://www.ready.noaa.gov>), driven by meteorological data from NCEP Global Data Assimilation System (GDAS) model at 0.5° resolution<sup>53</sup>.

### Analysis and statistics

Optical identification of bioaerosols was performed using the morphological characters, as referenced in the literature<sup>54–58</sup>. For sampling, a sticky clear tape was used to continuously collect particles from 5 to 500 µm in size in a steady flow of 10 LPM (liters per minute). This type of sampler collects the large particles within the air flow that attach to the surface of the adhesive tape<sup>59</sup>, which might not correspond to 100% of the particles present in the air flow in the specified size range. Each 48 mm of the tapes were mounted onto glass slides with a coverslip (corresponding to 24 h of sampling) and longitudinal analyzed by optical microscopy using an Olympus BX50 light microscope (Fig. 6). The brightfield optics equipment utilized an Olympus UPlanApo lens (40x) allowing a 400x image magnification, with images taken by a Canon EOS 1100D camera coupled to the microscope.

Particles were identified in 240 fields of view for each glass slide, i.e., 10 sequential fields of view each 2 mm, corresponding to 1-h sample, following the guidelines from the International Association for Aerobiology<sup>3,35</sup>. Identification and counting were performed both manually (to distinguish between the different particle types), and by the open source software Image J (NIH—USA, version 1.51j8), which was also used for size measurements. The results were processed using 1-h resolution, and particle concentrations were calculated using the number of particles according to the respective volume of sampled air.

A total of 495,906 particles with the size range of 5 to 500 µm were counted, measured and categorized. The PBA particles<sup>2</sup> were separated into the following categories: (a) pollens grains, (b) fungal spores, (c) yeasts-like conidia, (d) fern spores, (e) bryophyte

spores, and (f) canopy debris (including leaf/wood pieces, plant waxes, leaf glands, leaf trichomes, insect fragments). Another category defined as other particles includes all the remaining material not identified as biological, such as framework silicates and amorphous particles (Fig. 6).

Each sampling and analysis is susceptible to random and systematic errors related to equipment functioning and human operation. In this context, the uncertainty for the sampling (sampler efficiency, flow deviation) and analysis (particle counts) of 19.5% was calculated at the 95% level of confidence<sup>60</sup>. This uncertainty was considered for the values presented in the results. The distribution of particle concentrations did not fit a Gaussian curve; therefore, all valid measured data were statistically analyzed using non-parametric tests of the R software (The R Project—Austria, version 3.3.3). The R packages ggplot2, openair and RColorBrewer were used for figures. Hourly PBA concentrations were related to meteorological data using Spearman Rank analysis, GLM and GAM tests. The Mann–Whitney test was performed for both seasons among the heights and applied to test day/night differences. Data were considered statistically significant at  $p < 0.01$  and a 99% level of confidence.

## DATA AVAILABILITY

The data that support the findings of this study are available within the paper, supplementary information files, and data repositories. Details about the method optimization are available in “Zenodo” with the identifier “doi:10.5281/zenodo.5178552”. Image atlas for the sampled bioaerosol particles available in “figshare” with the identifier “doi: 10.6084/m9.figshare.15142419”. And the PBA data presented is available at the ATTO Data Portal <https://www.attodata.org/> with the identifier “Id330: Giant Bioaerosol Particles over the rainforest (2015–2019)”.

Received: 24 February 2022; Accepted: 30 August 2022;

Published online: 16 September 2022

## REFERENCES

1. Ben-Ami, Y. et al. Transport of North African dust from the Bodélé depression to the Amazon Basin: a case study. *Atmos. Chem. Phys.* **10**, 7533–7544 (2010).
2. Després, V. et al. Primary biological aerosol particles in the atmosphere: a review. *Tellus B Chem. Phys. Meteorol.* **64**, 15598 (2012).
3. Elbert, W., Taylor, P. E., Andreae, M. O. & Pöschl, U. Contribution of fungi to primary biogenic aerosols in the atmosphere: wet and dry discharged spores, carbohydrates, and inorganic ions. *Atmos. Chem. Phys.* **7**, 4569–4588 (2007).
4. Fröhlich-Nowoisky, J. et al. Bioaerosols in the earth system: climate, health, and ecosystem interactions. *Atmos. Res.* **182**, 346–376 (2016).
5. Huffman, J. A. et al. Size distributions and temporal variations of biological aerosol particles in the Amazon rainforest characterized by microscopy and real-time UV-APS fluorescence techniques during AMAZE-08. *Atmos. Chem. Phys.* **12**, 11997–12019 (2012).
6. Andreae, M. O. & Crutzen, P. J. Atmospheric aerosols: biogeochemical sources and role in atmospheric chemistry. *Science* **276**, 1052–1058 (1997).
7. Martin, S. T. et al. Sources and properties of Amazonian aerosol particles. *Rev. Geophys.* **48**, RG2002 (2010).
8. Andreae, M. O. et al. The Amazon Tall Tower Observatory (ATTO): overview of pilot measurements on ecosystem ecology, meteorology, trace gases, and aerosols. *Atmos. Chem. Phys.* **15**, 10723–10776 (2015).
9. Prass, M. et al. Bioaerosols in the Amazon rain forest: temporal variations and vertical profiles of Eukarya, Bacteria, and Archaea. *Biogeosciences* **18**, 4873–4887 (2021).
10. Pöhlker, C. et al. Efflorescence upon humidification? X-ray microspectroscopic in situ observation of changes in aerosol microstructure and phase state upon hydration. *Geophys. Res. Lett.* **41**, 3681–3689 (2014).
11. Saturno, J. et al. Black and brown carbon over central Amazonia: long-term aerosol measurements at the ATTO site. *Atmos. Chem. Phys.* **18**, 12817–12843 (2018).
12. Pöhlker, M. L. et al. Long-term observations of cloud condensation nuclei over the Amazon rain forest—Part 2: variability and characteristics of biomass burning, long-range transport, and pristine rain forest aerosols. *Atmos. Chem. Phys.* **18**, 10289–10331 (2018).
13. Schrod, J. et al. Long-term deposition and condensation ice-nucleating particle measurements from four stations across the globe. *Atmos. Chem. Phys.* **20**, 15983–16006 (2020).
14. China, S. et al. Fungal spores as a source of sodium salt particles in the Amazon Basin. *Nat. Commun.* **9**, 4793 (2018).
15. Ramsay, R. et al. Concentrations and biosphere–atmosphere fluxes of inorganic trace gases and associated ionic aerosol counterparts over the Amazon rainforest. *Atmos. Chem. Phys.* **20**, 15551–15584 (2020).
16. Langenbrunner, B., Pritchard, M. S., Kooperman, G. J. & Randerson, J. T. Why does Amazon precipitation decrease when tropical forests respond to increasing CO<sub>2</sub>? *Earth's Futur* **7**, 450–468 (2019).
17. Silva Dias, M. A. F. Cloud and rain processes in a biosphere-atmosphere interaction context in the Amazon region. *J. Geophys. Res.* **107**, 8072 (2002).
18. Arraut, J. M., Nobre, C., Barbosa, H. M. J., Obregon, G. & Marengo, J. Aerial rivers and lakes: looking at large-scale moisture transport and its relation to amazonia and to subtropical rainfall in South America. *J. Clim.* **25**, 543–556 (2012).
19. Nobre, C. A., Obregón, G. O., Marengo, J. A., Fu, R. & Poveda, G. In *Amazonia and Global Change* (eds. Keller, M. et al.) 149–162 (Geophysical Monograph Series, 2009).
20. Pope, F. D. Pollen grains are efficient cloud condensation nuclei. *Environ. Res. Lett.* **5**, 044015 (2010).
21. Posselt, R. & Lohmann, U. Influence of Giant CCN on warm rain processes in the ECHAM5 GCM. *Atmos. Chem. Phys.* **8**, 3769–3788 (2008).
22. Mechem, D. B. & Kogan, Y. L. A bulk parameterization of giant CCN. *J. Atmos. Sci.* **65**, 2458–2466 (2008).
23. Campbell, I. D., McDonald, K., Flannigan, M. D. & Kringayark, J. Long-distance transport of pollen into the Arctic. *Nature* **399**, 29–30 (1999).
24. Rizzolo, J. A. et al. Soluble iron nutrients in Saharan dust over the central Amazon rainforest. *Atmos. Chem. Phys.* **17**, 2673–2687 (2017).
25. Raynor, G. S., Ogden, E. C. & Hayes, J. V. Variation in ragweed pollen concentration to a height of 108 meters. *J. Allergy Clin. Immunol.* **51**, 199–207 (1973).
26. Mandrioli, P., Negrini, M. G., Cesari, G. & Morgan, G. Evidence for long range transport of biological and anthropogenic aerosol particles in the atmosphere. *Grana* **23**, 43–53 (1984).
27. Hart, M. L., Wentworth, J. E. & Bailey, J. P. The effects of trap height and weather variables on recorded pollen concentration at leicester. *Grana* **33**, 100–103 (1994).
28. Sofiev, M., Siljamo, P., Ranta, H. & Rantio-Lehtimäki, A. Towards numerical forecasting of long-range air transport of birch pollen: theoretical considerations and a feasibility study. *Int. J. Biometeorol.* **50**, 392–402 (2006).
29. Womack, A. M. et al. Characterization of active and total fungal communities in the atmosphere over the Amazon rainforest. *Biogeosciences* **12**, 6337–6349 (2015).
30. Damialis, A. et al. Estimating the abundance of airborne pollen and fungal spores at variable elevations using an aircraft: How high can they fly? *Sci. Rep.* **7**, 44535 (2017).
31. Celenk, S. Detection of reactive allergens in long-distance transported pollen grains: evidence from ambrosia. *Atmos. Environ.* **209**, 212–219 (2019).
32. Hassett, M. O., Fischer, M. W. F. & Money, N. P. Mushrooms as rainmakers: how spores act as nuclei for raindrops. *PLoS One* **10**, 1–10 (2015).
33. Pöhlker, C. et al. Biogenic potassium salt particles as seeds for secondary organic Aerosol in the Amazon. *Science* **337**, 1075–1078 (2012).
34. Barbosa, C., Taylor, P. & Godoi, R. H. M. ATLAS—Bioaerosols from the Brazilian Amazon rainforest: pollens and spores. *Figshare* <https://doi.org/10.6084/m9.figshare.15142419.v1> (2021).
35. Colinvaux, P. A., Oliveira, P. E. & Patino, J. E. M. *Amazon Pollen Manual and Atlas*. (Taylor & Francis, Amsterdam, 2005).
36. Taylor, P. E., Card, G., House, J., Dickinson, M. H. & Flagan, R. C. High-speed pollen release in the white mulberry tree, *Morus alba* L. *Sex. Plant Reprod.* **19**, 19–24 (2006).
37. Taylor, P. E., Flagan, R. C., Valenta, R. & Glovsky, M. M. Release of allergens as respirable aerosols: a link between grass pollen and asthma. *J. Allergy Clin. Immunol.* **109**, 51–56 (2002).
38. Taylor, P. E., Flagan, R. C., Miguel, A. G., Valenta, R. & Glovsky, M. M. Birch pollen rupture and the release of aerosols of respirable allergens. *Clin. Exp. Allergy* **34**, 1591–1596 (2004).
39. Mikhailov, E. F. et al. Water uptake of subpollen aerosol particles: Hygroscopic growth, cloud condensation nuclei activation, and liquid-liquid phase separation. *Atmos. Chem. Phys.* **21**, 6999–7022 (2021).
40. Steiner, A. L. et al. Pollen as atmospheric cloud condensation nuclei. *Geophys. Res. Lett.* **42**, 3596–3602 (2015).
41. Wozniak, M. C., Solmon, F. & Steiner, A. L. Pollen rupture and its impact on precipitation in clean continental conditions. *Geophys. Res. Lett.* **45**, 7156–7164 (2018).

42. Hughes, D. D., Mampage, C. B. A., Jones, L. M., Liu, Z. & Stone, E. A. Characterization of atmospheric pollen fragments during springtime thunderstorms. *Environ. Sci. Technol. Lett.* **7**, 409–414 (2020).
43. Graham, B. et al. Organic compounds present in the natural Amazonian aerosol: Characterization by gas chromatography-mass spectrometry. *J. Geophys. Res. Atmos.* **108**, 1–13 (2003).
44. Chor, T. L. et al. Flux-variance and flux-gradient relationships in the roughness sublayer over the Amazon forest. *Agric. Meteorol.* **239**, 213–222 (2017).
45. Chamecki, M. et al. Effects of vegetation and topography on the boundary layer structure above the Amazon forest. *J. Atmos. Sci.* **77**, 2941–2957 (2020).
46. Pöhlker, C. et al. Land cover and its transformation in the backward trajectory footprint region of the Amazon tall tower observatory. *Atmos. Chem. Phys.* **19**, 8425–8470 (2019).
47. Moran-Zuloaga, D. et al. Long-term study on coarse mode aerosols in the Amazon rain forest with the frequent intrusion of Saharan dust plumes. *Atmos. Chem. Phys.* **18**, 10055–10088 (2018).
48. Huffman, J. A. et al. High concentrations of biological aerosol particles and ice nuclei during and after rain. *Atmos. Chem. Phys.* **13**, 6151–6164 (2013).
49. Cardelús, C. L., Mack, M. C., Woods, C., Demarco, J. & Treseder, K. K. The influence of tree species on canopy soil nutrient status in a tropical lowland wet forest in Costa Rica. *Plant Soil* **318**, 47–61 (2009).
50. Jantz, N., Homeier, J., León-Yáñez, S., Moscoso, A. & Behling, H. Trapping pollen in the tropics—comparing modern pollen rain spectra of different pollen traps and surface samples across Andean vegetation zones. *Rev. Palaeobot. Palynol.* **193**, 57–69 (2013).
51. Boehm, G. In *Advances in Aerobiology* (eds. Boehm, G. & Leuschner, R. M.) 377–379 (Birkhäuser, Basel, 1987).
52. Machado, L. A. T. et al. Overview: Precipitation characteristics and sensitivities to environmental conditions during GoAmazon2014/5 and ACRIDICON-CHUVA. *Atmos. Chem. Phys.* **18**, 6461–6482 (2018).
53. Stein, A. F. et al. NOAA's hyssplit atmospheric transport and dispersion modeling system. *Bull. Am. Meteorol. Soc.* **96**, 2059–2078 (2015).
54. Kapp, R. O. *How to Know Pollen and Spores* (Wm. C. Brown Company, 1975).
55. Frenz, D. & Johann, J. *An Introduction to Sampling and Identifying Airborne Pollen and Fungus Spores* (Multidata LLC, 2001).
56. Kagen, S., Lewis, W. & Levetin, E. *The Classic Collection Transcribed. Aeroallergen PhotoLibrary of North America* (DePass Media Productions, 2005).
57. Lacey, M. E. & West, J. S. *The Air Spora* (Springer, 2006).
58. Caulton, E. et al. *Airborne Pollen and Spores: A Guide Do Trapping And Counting* (British Aerobiology Federation, 1995).
59. Barbosa, C. & Taylor, P. Adhesive optimization for bioaerosol sampling above the Amazon rainforest using a hirst-type volumetric trap. *Mol. Ecol. Resour.* <https://doi.org/10.5281/zenodo.5178552> (2021).
60. JCGM, J. C. F. G. I. M. Evaluation of measurement data—Guide to the expression of uncertainty in measurement. *Int. Organ. Stand. Geneva ISBN* **50**, 134 (2008).

## ACKNOWLEDGEMENTS

We acknowledge logistical support from the Central Office of the Large-Scale Biosphere-Atmosphere Experiment in Amazonia (LBA), the Instituto Nacional de Pesquisas da Amazônia (INPA), and the Universidade do Estado do Amazonas (UEA). We also thank the Max Planck Society and INPA for continuous support. For the operation of the ATTO site, we acknowledge the support by the German Federal Ministry of Education and Research (BMBF contract nos. 01LB1001A and 01LK1602B) and the Brazilian Ministério da Ciência, Tecnologia e Inovação (MCTI/FINEP contract 01.11.01248.00) as well as the SDS/CEUC/RDS-Uatumã. We acknowledge the support of the Reserva de Desenvolvimento Sustentável Uatumã (SDS/CEUC/RDS-Uatumã), Fundação de Amparo à Pesquisa do Estado do Amazonas (FAPEAM), Financiadora de

Estudos e Projetos (FINEP), Coordenação de Aperfeiçoamento de Pessoal de Nível Superior (CAPES), Conselho Nacional de Desenvolvimento Científico e Tecnológico (CNPq), and the Fundação Araucária de Apoio ao Desenvolvimento Científico e Tecnológico do Paraná (FA). The opinions expressed here are the entire responsibility of the authors and not of the participating institutions. C.G.G.B. would like to thank CAPES for the funding to execute analysis at Deakin University, Australia (CAPES 88881.134401/2016-01), the NARL lab in the person of Dr. Cenk Suphioglu, also Anna Withanage, Emma Blanchonette and Sam King for the lab support, and Guilherme Borillo for the analysis support. We would like to especially thank all the people involved in the logistical support of the ATTO project, and the field staff, specially Nagib Alberto and Antonio Huxley for the support during sampling.

## AUTHOR CONTRIBUTIONS

C.G.G.B., R.A.F.S., B.S. executed sampling, C.G.G.B., P.E.T. carried out sample analysis, M.O.S., P.R.T., R.I.A., H.M.J.B., A.C.A. provided meteorological data, A.O.M., C.P., S.M.O., B.W., M.O.A., M.P., R.H.M.G. helped with data analysis. All authors commented on the paper.

## FUNDING

Open Access funding enabled and organized by Projekt DEAL.

## COMPETING INTERESTS

The authors declare no competing interests.

## ADDITIONAL INFORMATION

**Supplementary information** The online version contains supplementary material available at <https://doi.org/10.1038/s41612-022-00294-y>.

**Correspondence** and requests for materials should be addressed to Cybelli G. G. Barbosa or Ricardo H. M. Godoi.

**Reprints and permission information** is available at <http://www.nature.com/reprints>

**Publisher's note** Springer Nature remains neutral with regard to jurisdictional claims in published maps and institutional affiliations.



**Open Access** This article is licensed under a Creative Commons Attribution 4.0 International License, which permits use, sharing, adaptation, distribution and reproduction in any medium or format, as long as you give appropriate credit to the original author(s) and the source, provide a link to the Creative Commons license, and indicate if changes were made. The images or other third party material in this article are included in the article's Creative Commons license, unless indicated otherwise in a credit line to the material. If material is not included in the article's Creative Commons license and your intended use is not permitted by statutory regulation or exceeds the permitted use, you will need to obtain permission directly from the copyright holder. To view a copy of this license, visit <http://creativecommons.org/licenses/by/4.0/>.

© The Author(s) 2022